Effects of 3D basin structure on long-period ground motions in SW British Columbia, Canada, for large scenario earthquakes

S. Molnar
University of British Columbia, Vancouver, BC, Canada

J.F. Cassidy & Jiangheng He
Natural Resources Canada, Sidney, BC, Canada

K.B. Olsen
San Diego State University, San Diego, U.S.A.

S.E. Dosso
University of Victoria, Victoria, BC, Canada

15 WCEE
LISBOA 2012

SUMMARY:
Finite-difference modeling of 3D viscoelastic wave propagation for large (M_W 6.8) scenario earthquakes is conducted to investigate effects of the Georgia basin structure on long-period (> 2 s) ground shaking in Greater Vancouver, British Columbia, Canada. This research provides the first detailed investigation of 3D earthquake ground motion for a sedimentary basin in Canada. The region of greatest seismic risk in the country is the Greater Vancouver area with critical infrastructure and a population of >2 million located at the northern end of the Cascadia subduction zone. The Georgia basin is a northwest-oriented structural depression that extends from southwestern British Columbia southward into Washington State, with Tertiary dimensions of 130 by 70 by 5 km. Scenario earthquakes include shallow (5 km) and deep (> 40 km) events within the over-riding North America (NA) and subducting Juan de Fuca (JdF) plates, respectively, simulated in locations congruent with known seismicity within 100 km of Greater Vancouver. Two sets of simulations are performed for a given scenario earthquake using 3D physical-structure models with and without basin sediments. The ratio between predicted peak ground velocity for the two simulations is applied here as a quantitative measure of amplification due to 3D basin structure. Simulations are calibrated using records from the 2001 M_W 6.8 Nisqually earthquake. For all simulations, some general effects are observed consistently when Georgia basin sediments are included in the 3D structure model: the symmetry of the seismic radiation pattern is distorted, the area of higher ground motions is increased, and the highest onshore basin amplification occurs in a localized region of southern Greater Vancouver from the focusing of surface waves due to shallow (< 1 km) basin structure. Deep JdF plate scenario earthquakes are simulated in 10 different locations; the predicted average maximum peak ground velocity and basin amplification at stiff soil sites across Greater Vancouver is ~6 cm/s (intensity V) and a factor of ~2.5, respectively. From simulations of shallow NA plate scenario earthquakes in 9 different locations, the corresponding average values are ~30 cm/s (intensity VII-VIII) and a factor of ~3, respectively. Overall, this study shows that the presence of 3D Georgia basin structure increases the level of predicted long-period ground shaking.

Keywords: 3D basin effects, ground motion simulation, finite-difference modelling, amplification

1. INTRODUCTION

This paper presents finite difference (FD) simulations of long-period (> 2 s) ground motions computed for scenario earthquakes in SW British Columbia in a regional 3D velocity model of the Georgia basin. This research provides the first detailed investigation of 3D earthquake ground motion for a sedimentary basin in Canada. The main objective here is to examine the effect of 3D Georgia basin structure on predicted ground shaking across Greater Vancouver from large (M_W 6.8) scenario earthquakes. The Georgia basin is a NW-oriented Late-Cretaceous structural depression that extends predominantly E across Georgia Strait to mid-Vancouver Island and S into mainland Washington state, and is relatively wide and shallow (Tertiary dimensions of 130 by 70 by 5 km). Figure 1 displays the historical and recorded seismicity of the two types of scenario earthquakes investigated here: (1) deep (42-55 km) events in the subducting Juan de Fuca (JdF) plate, which are based on the rupture of the normal-faulting 2001 M_W 6.8 Nisqually, WA, earthquake; and (2) shallow (5 km) events in the North America (NA) plate, which are based on the rupture of the blind-thrust 1994 M_W 6.7 Northridge, CA, earthquake. Scenario earthquakes are simulated in different epicentral locations in the Georgia basin region, congruent with known seismicity and within 100 km of Vancouver, to investigate variation in the strength of predicted ground motions and 3D basin effects. The peak ground velocity (PGV) metric chosen here is the square-root-sum-of-squares of the three components of motion, calculated as

$$\mathrm{PGV} = \max_t(\mathrm{sqrt}[v_{EW}(t)^2+v_{NS}(t)^2+v_{UD}(t)^2]), \tag{1.1}$$

where $v(t)$ represents a synthetic velocity waveform. Amplification due to basin structure is evaluated as the ratio of peak motion from simulations of the same scenario earthquake in 3D basin and non-basin structure models, as performed for the Los Angeles basin by Olsen (2000). In order to conduct this research, the Georgia basin 3D structure model is revised with recent geological and geophysical information and calibrated by simulating the Nisqually earthquake and comparing the synthetic results to recordings. Limitations of this work include: (1) uncertainty in physical-structure and source-rupture models, (2) omission of low-velocity material (e.g. water and up to 300 m of Holocene sediments) and surface topography in the physical structure models, and (3) inability to resolve frequencies > 0.5 Hz. Nonetheless, the work presented here represents an important first step towards quantifying the effect of the 3D sedimentary Georgia basin structure on earthquake ground motion in SW British Columbia. This work is summarized from Molnar (2011) and Molnar et al. (2012a,b).

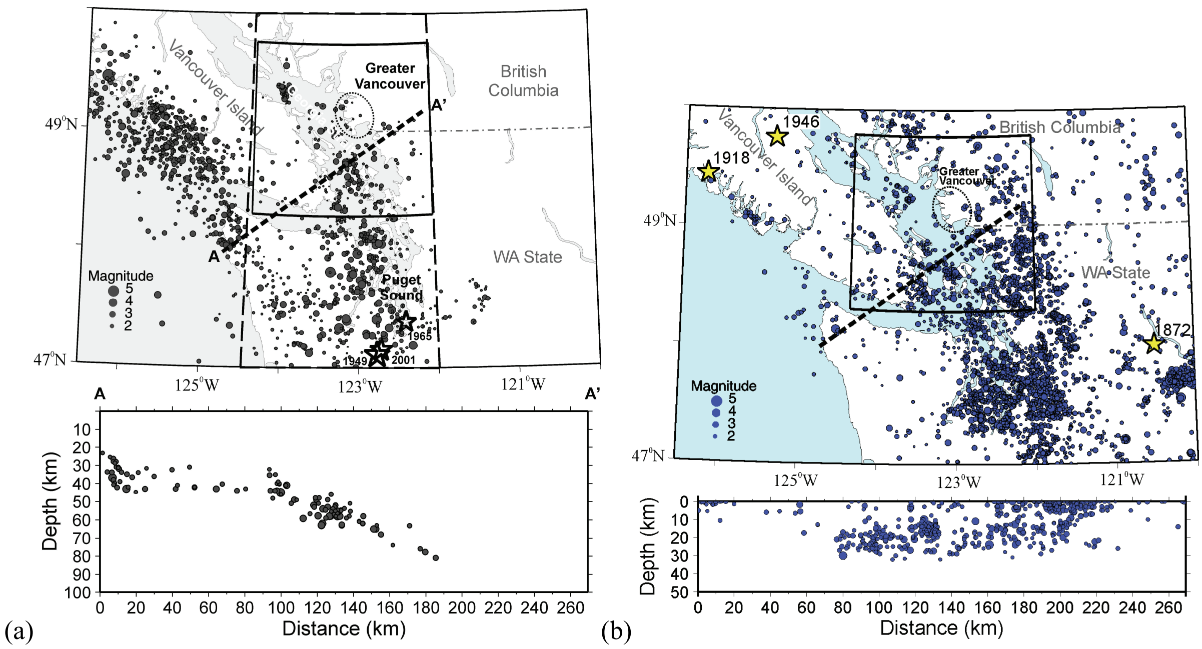

Figure 2. Seismicity maps (1985-1999) of (a) deep JdF plate events and (b) shallow NA plate events. Significant (and/or large historical) earthquakes (M > 6) represented by stars and labeled by year. Limits of the Georgia basin regional model shown by solid box and Pacific NW model shown by dashed box in (a) only. Greater Vancouver is bounded by dotted ellipse. Thick dashed line denotes seismic cross-section shown in bottom panels (M 2 minimum).

1.1. Physical structure models

The base elastic 3D model is extracted from the Stephenson (2007) Pacific NW 3D velocity model. Two different sizes of physical structure models are used; a Pacific NW model that spans from NW Washington to SW British Columbia is used for simulation of the Nisqually earthquake at > 150 km from Greater Vancouver, and a smaller regional model is used for simulations of scenario earthquakes within 100 km of Greater Vancouver. For the FD simulations carried out in this paper, the upper 1 km of the base elastic 3D model is updated in the Georgia basin region of SW British Columbia. The minimum shear-wave velocity, V_S, is set to 625 m/s for computational feasibility. In S Greater

Vancouver, up to 300 m of Holocene deltaic sediments of the Fraser River are effectively ignored, i.e. represented by a V_S of 625 m/s. The surface of the 3D basin model therefore represents over-consolidated Pleistocene glacial sediments or stiff soil sites. This is a significant limitation to modeling of the potential earthquake ground motion here, and the overall amplitude and duration of simulated ground motions in the Georgia basin are likely biased. The V_P/V_S ratio is set to 2 for $V_P \leq 5.5$ km/s in the updated 3D basin model; the base of the Georgia basin is composed of Late-Cretaceous Nanaimo Group rocks, inferred as the 5.5-6.0 km/s V_P surface in regional tomographic V_P models. This higher V_P limit for the V_P/V_S ratio of 2 effectively causes low V_S values to extend to greater depths in the updated model. Surface topography is not included.

A non-basin 3D model is also generated from the updated basin model by setting the minimum compressional-wave velocity, V_P, to 5.5 km/s, effectively replacing basin sediments with inferred basement. The non-basin velocity model is based on the typical 1D velocity profile for rock sites in SW British Columbia. Figure 2 compares the surface (0-250 m) depth surface of the updated basin and non-basin regional models. The maximum depth of the Georgia basin is 6.5 km at its SE extent; hence, the basin and non-basin models are identical below 6.5 km depth. For the same scenario earthquake, the ratio of peak motions predicted using the basin and non-basin models provide a quantitative measure of 3D Georgia basin effects.

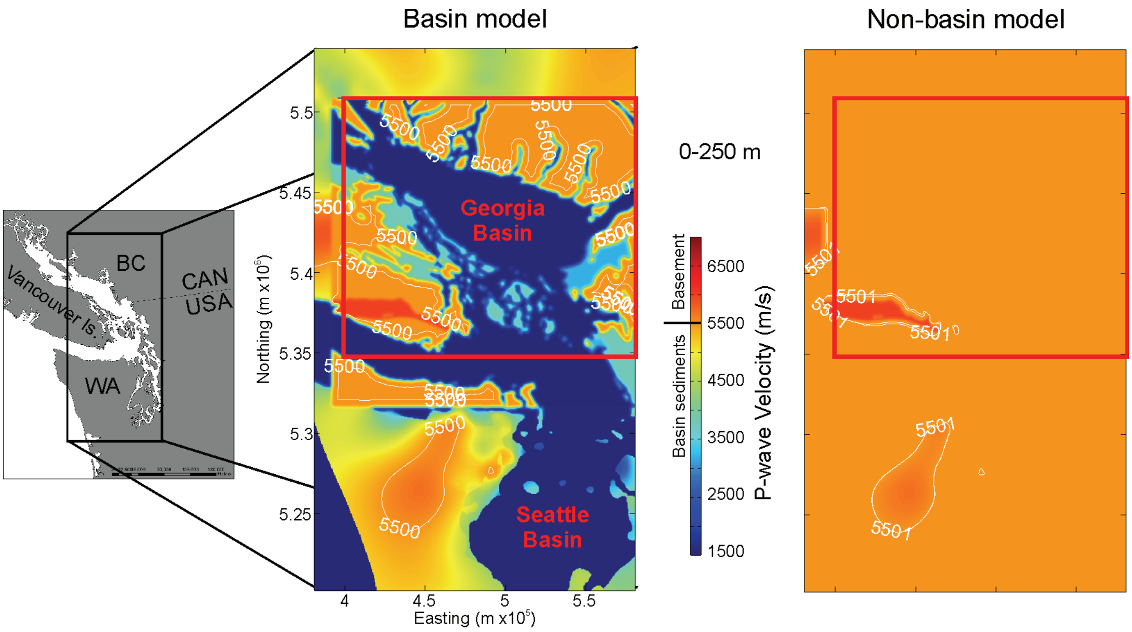

Figure 2. Surface (0-250 m) depth slices of the basin and non-basin Pacific NW V_P models. Red box outlines limits of the Georgia basin regional V_P model.

1.2. Finite difference scheme

The 3D elastic equations of wave motion are solved here using the FD scheme of Olsen (1994) with fourth-order accuracy in space and second-order accuracy in time. The physical model is represented by a uniform cubic mesh discretized with a spacing equivalent to 5 nodes per minimum shear wavelength, which limits the maximum resolvable frequency. In this work, the uniform grid size of the physical model is 250 m with a minimum V_S of 625 m/s, such that the maximum resolvable frequency is 0.5 Hz (2 s period). Viscoelasticity is incorporated independently for P and S waves using a coarse-grained implementation of the memory variables. The Q relations of Frankel et al. (2009) for stiff sediments in the Pacific NW are the most geologically reasonable and are assigned here: for $V_S < 1000$ m/s, $Q_S = 0.1643 \times V_S - 14$; for $V_S > 1000$ m/s, $Q_S = 0.15 \times V_S$; and $Q_P = 2 \times Q_S$. Overall, Q_S increases from 89 at the surface to 723 at 60 km depth in the updated 3D basin model. The seismic source is implemented in the FD grid by subtracting $M_{ij}(t)/V$ from $S_{ij}(t)$ where $M_{ij}(t)$ is the ijth component of the moment tensor for the earthquake, $V = dx^3$ is the cell volume, and $S_{ij}(t)$ is the *ij*th component of the stress tensor on the fault at time *t*.

1.3 Accuracy of the simulations

Accuracy of the 3D FD simulations are evaluated by comparing predicted and empirical waveforms of the 2001 M_W 6.8 Nisqually earthquake, which is currently the only large high-quality empirical dataset available for the Georgia basin region. General agreement in amplitude and phase of first arrival S-waves is obtained at stations in the Seattle basin within 100 km of the source; the Nisqually earthquake source-rupture model is relatively well determined from previous 3D FD simulation studies (Pitarka et al. 2004; Frankel et al. 2007; 2009). In this near-source region, estimates of PGV (0.2-0.4 Hz bandwidth) are biased upward by a factor of 1.3. For the Georgia basin region, the bias between predicted and empirical PGV is a factor of 2.1, which is reduced to a factor of 1.6 when the base Pacific NW velocity model is updated here with higher-resolution shallow (< 1 km) geologic and geophysical datasets. Improvement in predicted low frequency ground motions is negligible for a variety of physically reasonable Q relations for the lowest velocity sediments in the basin model. Overall, general agreement of waveforms in the near-source region is achieved and provides confidence in the use of the Nisqually earthquake source model to simulate large subducting JdF plate scenario earthquakes in the Georgia basin region.

2. DEEP M_W 6.8 JDF PLATE SCENARIO EARTHQUAKES

The goal is to quantify the 3D Georgia basin effect on long-period ground shaking in Greater Vancouver for realistic scenarios of M_W 6.8 JdF plate earthquakes. Figure 3 shows the epicenters of 10 scenario JdF plate earthquakes considered here, chosen in a 30-40 km grid-spacing spanning the Georgia basin region congruent with known seismicity (Figure 1). At each scenario earthquake location, the Nisqually earthquake source model is initiated near the top of the oceanic crust which subducts NE beneath Greater Vancouver; hence, the deepest earthquakes occur towards the NE. The maximum source depth is constrained to 55 km by the maximum 60 km depth of the regional velocity structure models. The most realistic scenarios are those along the extent of Georgia Strait for the chosen magnitude and depth limitations of the model (scenarios 1, 2, 6, 9 and 10); ground motions are likely biased upward for scenarios furthest NE (scenarios 3 and 4).

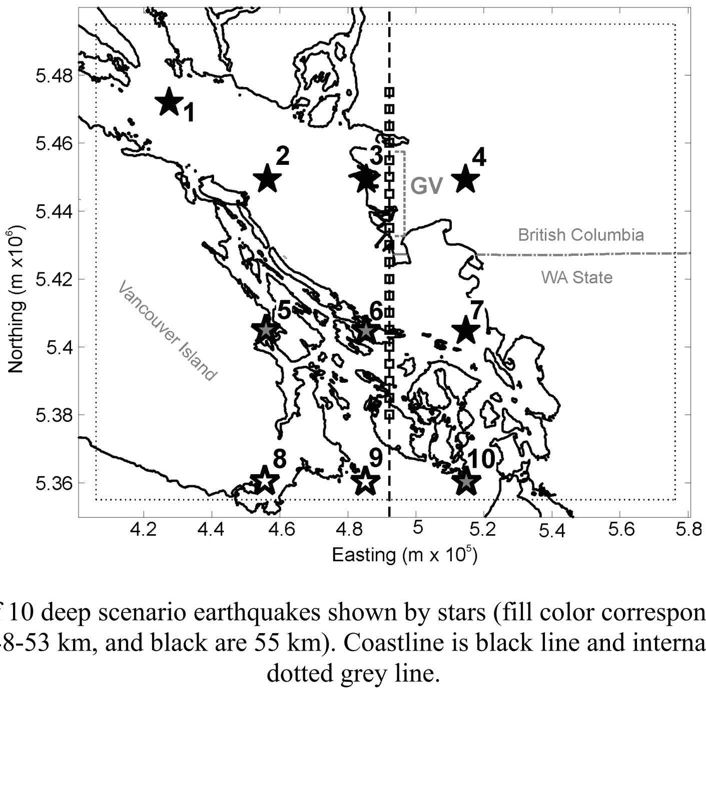

Figure 3. Epicenters of 10 deep scenario earthquakes shown by stars (fill color corresponds to focal depth: white are 42 km, grey are 48-53 km, and black are 55 km). Coastline is black line and international border is dash-dotted grey line.

Figure 4 shows PGV maps for all 10 scenarios; panel layout corresponds to the spatial distribution of scenario earthquake epicenters. Generally, higher ground motions occur W of the epicenter due to the source radiation pattern. The highest ground motions are coincident with the lowest velocity sediments in the upper 1 km of the model, although the level and spatial extent of ground shaking is unique to each scenario. The range in predicted maximum PGV in the Georgia basin region is 8.7 to 15.8 cm/s, corresponding to a shaking intensity of VI (Wald et al. 1999). Maximum PGV in Greater Vancouver ranges from 4.5 to 9.3 cm/s, predominantly intensity V, only reaching intensity VI (> 8.1 cm/s) when a deep JdF plate earthquake is located 25 km E (scenario #4) of the city. For context, the M_W 6.8 Nisqually earthquake produced long-period shaking levels ≤ 5 cm/s in the Seattle basin and resulted in $2 billion US dollars of damage in Washington.

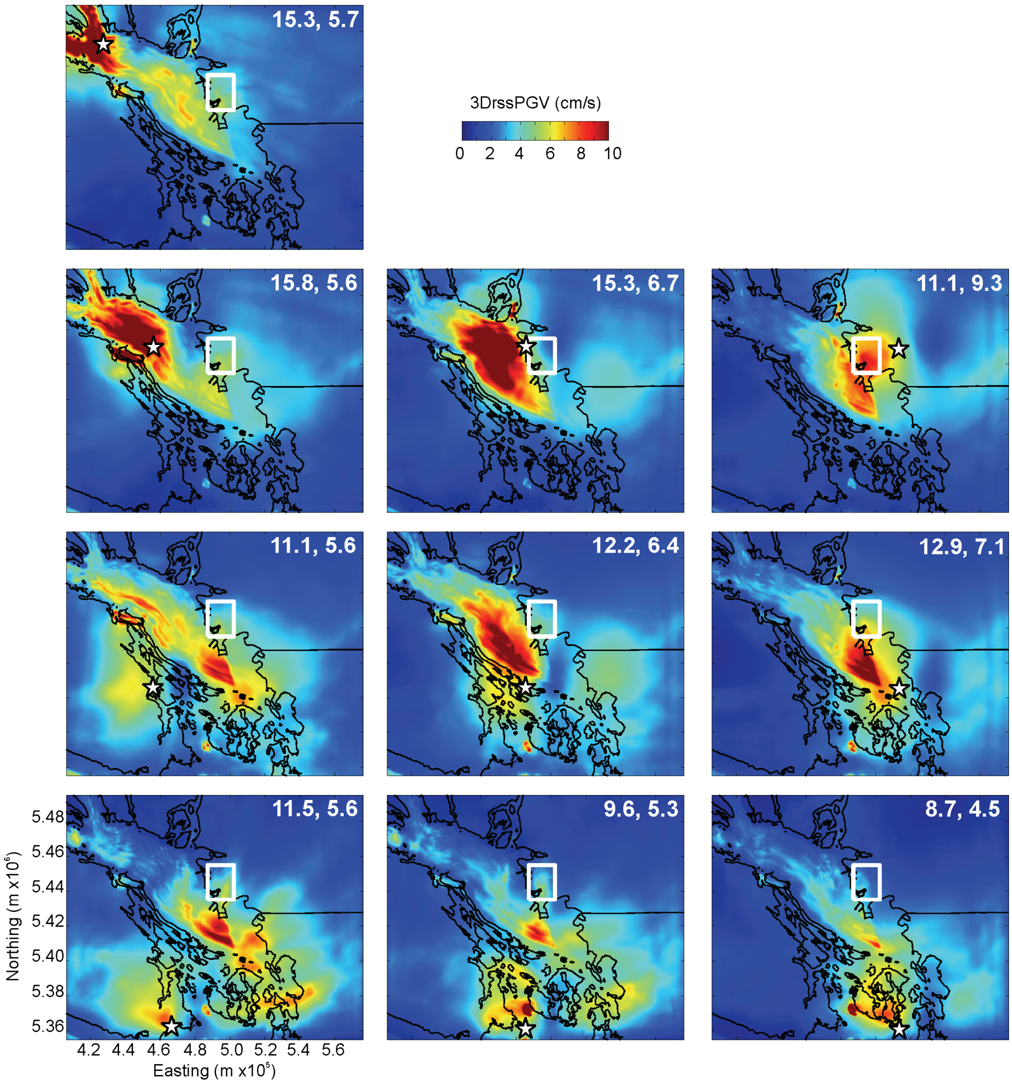

Figure 4. PGV (cm/s) for all 10 deep scenario earthquakes; stars show epicenters and coastline and the international border are shown by black lines. Numbers in upper right of each panel correspond to maximum PGV within the Georgia basin (map area shown north of 5.38 x10^6 m) and Greater Vancouver (white rectangle) regions.

Figure 5 shows basin amplification maps (ratio of PGV between basin and non-basin simulations) for the 10 scenario JdF plate earthquakes. As an example, the EW-component waveform at a selected location within Greater Vancouver is also shown in Figure 5 for the basin and non-basin model simulations of each scenario earthquake. The presence of the NW-oriented Georgia basin is readily apparent and is associated with amplification factors ≥ 2.5. The highest basin amplification (up to a factor of 7) generally occurs near each earthquake epicenter but is generally coincident with the lowest-velocity Georgia basin sediments in the upper 1 km. In Greater Vancouver, the highest ground motions are associated with the scenario earthquake 25 km E of the city (#4), but the highest basin amplification (factor of 3 to 4) is associated with scenario earthquakes located ≥ 80 km S-SW of the city (scenarios #8, 9 and 10) due to the occurrence of later-arriving surface waves in basin model waveforms.

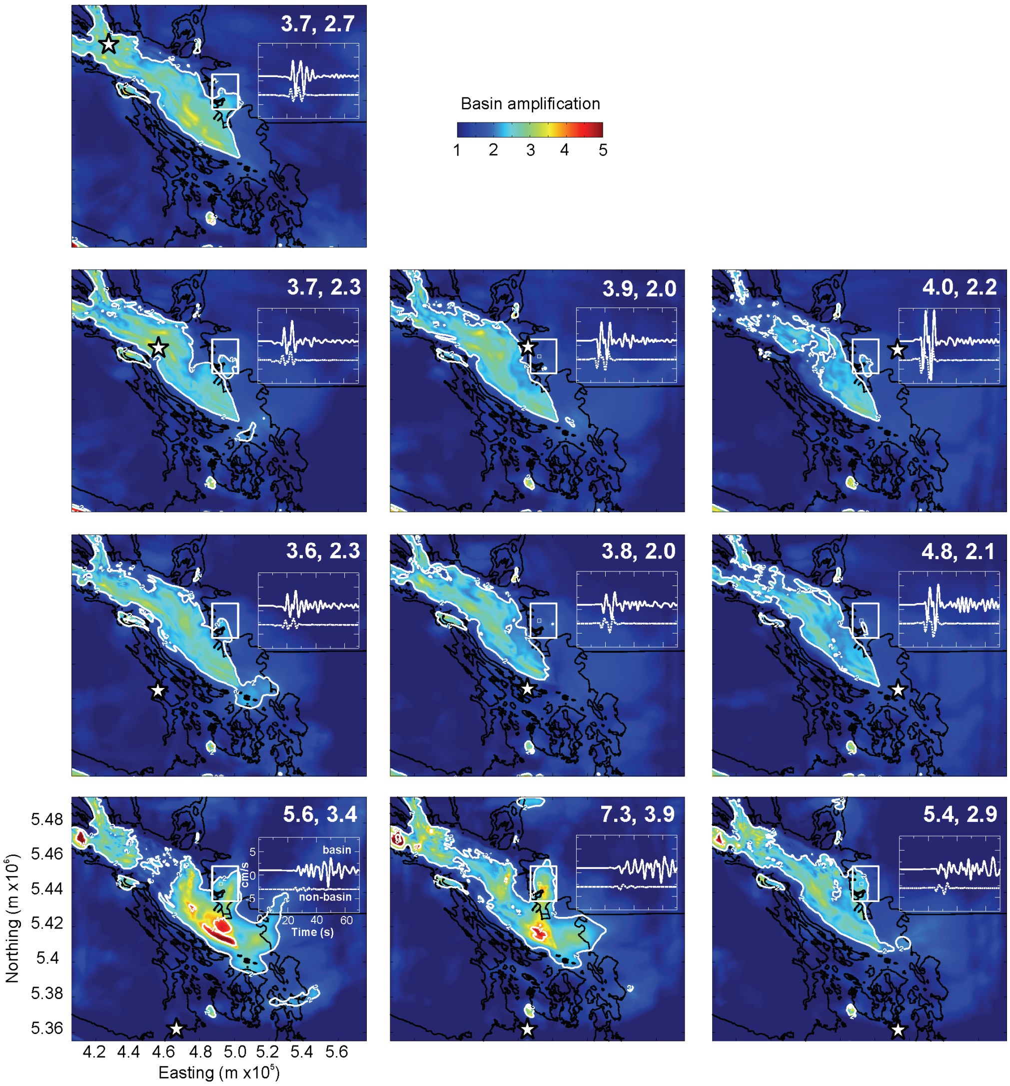

Figure 5. Basin amplification for all 10 deep scenario earthquakes (white lines denote contours of even-numbered factors); star shows epicenters and coastline and international border are shown by black lines. Numbers in upper right of each panel correspond to maximum basin amplification factor within the Georgia basin (map area shown north of 5.38 x10^6 m) and Greater Vancouver (white rectangle) regions. A synthetic EW-component waveform is shown for the basin (solid white line) and non-basin (dotted white line) model simulations corresponding to a location within Greater Vancouver (small white square).

A set of 10 deep scenario M_W 6.8 JdF plate earthquakes are simulated in Georgia basin and non-basin structure models to predict long-period ground motions in Greater Vancouver. Figure 6 presents maps of the average PGV and basin amplification of all 10 scenario earthquakes. These maps are considered to provide an estimate of the average peak motion and basin amplification related to a deep JdF plate earthquake within 100 km of Greater Vancouver. The presence of the Georgia basin significantly increases the level of predicted long-period ground motions. For the Georgia basin region as a whole, the average maximum PGV is 8.3 cm/s, related to an intensity of V-VI (Wald et al. 1999). The average maximum basin amplification is a factor of 3.4.

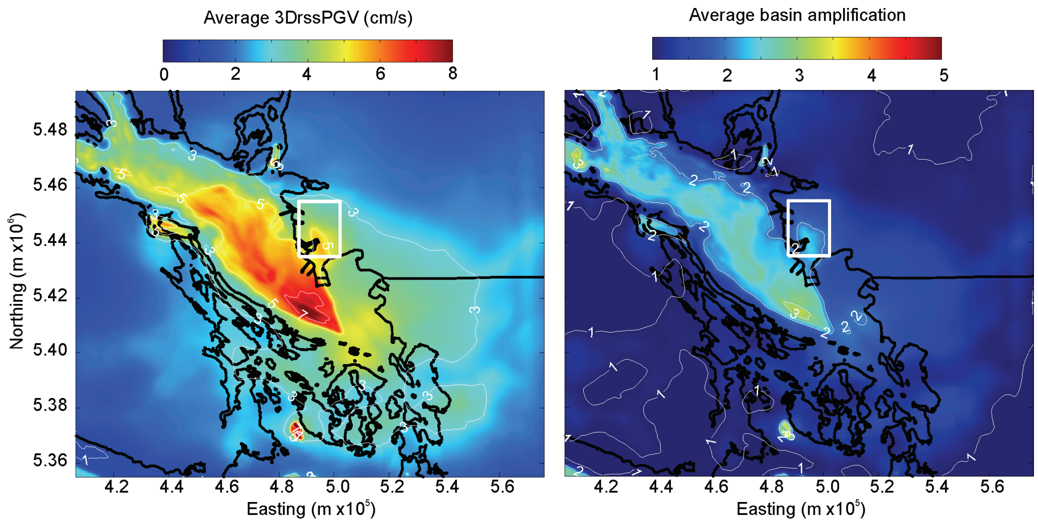

Figure 6. Average PGV (left panel) and basin amplification (right panel) of all 10 deep scenario earthquakes (white lines are contours of PGV (cm/s) and basin amplification factor, respectively). Coastline and the international border shown by black lines. Greater Vancouver is outlined by the white rectangle.

3. SHALLOW M_W 6.8 NA PLATE SCENARIO EARTHQUAKES

This section is focused on potential large shallow crustal NA plate earthquakes. No obvious correlation exists between mapped surface faults of the Georgia basin region and crustal NA plate earthquakes, and rupture characteristics of a large crustal NA plate earthquake are relatively unknown. The most comprehensive examination of fault-plane solutions from over 1000 NA plate earthquakes shows no dominant style of faulting; ~30% of faulting is strike-slip, thrust, or some combination thereof (Balfour et al. 2011). Linear clustering of recurrent shallow seismicity indicates potential "hidden" active faults and is the basis for locations of large shallow scenario events (Figure 7). Relocations of aftershock sequences predominantly align along EW-striking linear features that dip 53° to 60° N (Cassidy et al. 2000; Balfour et al. 2012) that temporally migrate downdip. Hence, the earthquake rupture model used to simulate large shallow scenario earthquakes here (Figure 7) is an EW-striking 45°-N dipping blind-thrust fault that ruptures downdip based on the kinematic model of the 1994 M_W 6.7 Northridge, CA, earthquake (Wald et al. 1996).

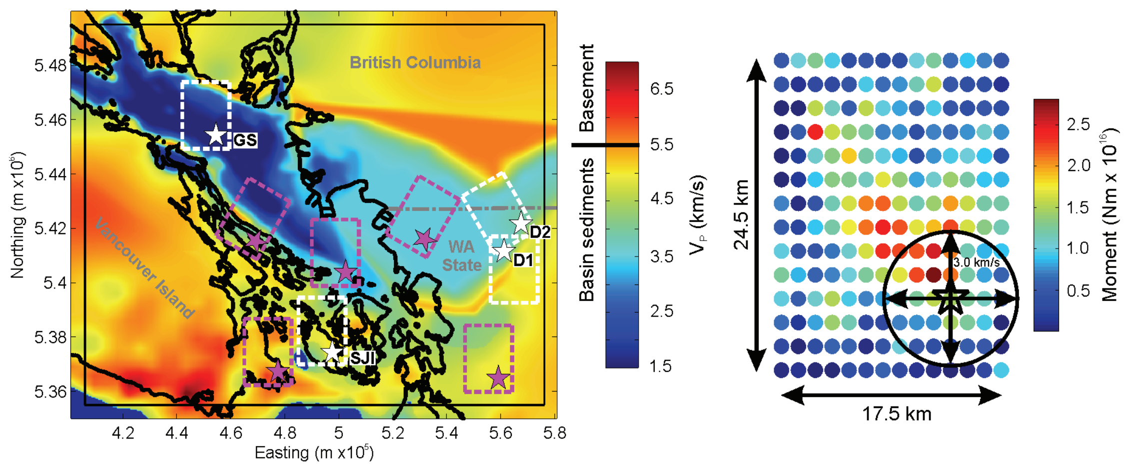

Figure 7. Left panel: Horizontal slice of basin V_P model at 500 m depth and shallow scenario earthquake epicenters (stars) and associated projected fault planes (dashed lines). Coastline is thick black line. Right panel: Colored circles correspond to locations of, and seismic moment associated with, each sub-fault; the entire fault plane is composed of 196 sub-faults. The 5-km deep focus is denoted by the star and ruptures at 3.0 km/s.

Figure 8 shows PGV maps for all 9 scenarios; panel layout corresponds to the spatial distribution of scenario earthquake epicenters. Generally, predicted ground motions are higher downdip (N) of each epicenter due to the source radiation pattern; hence, a scenario earthquake south of the city produces the highest ground motions (54.2 cm/s). The highest ground motions are coincident with the lowest velocity sediments in the upper 1 km of the model, although the level and spatial extent of ground shaking is unique to each scenario, similar to the deep scenario earthquake results. The average maximum PGV for a M_W 6.8 NA plate earthquake in the Georgia basin model is 70.4 cm/s (intensity IX). For the Greater Vancouver region, the average maximum PGV is 31.0 cm/s (intensity VII-VIII).

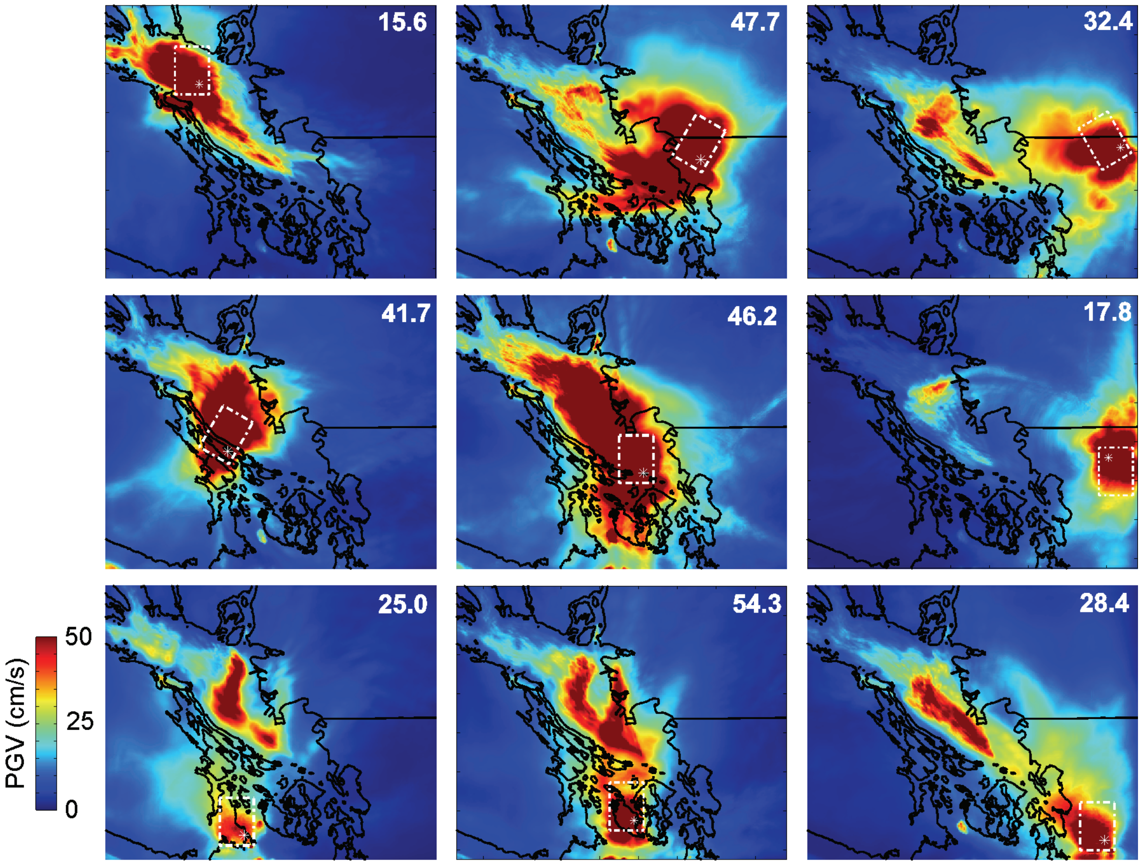

Figure 8. PGV (cm/s) for all 9 shallow scenario earthquakes. Number in upper right of each panel corresponds to maximum PGV within Greater Vancouver region.

Figure 9 shows basin amplification maps (ratio of PGV between basin and non-basin simulations) for the 9 shallow scenario earthquakes. As an example, the EW-component waveform at a selected location within Greater Vancouver is also shown in Figure 9 for the basin and non-basin model simulations of each scenario earthquake. The average maximum basin amplification factor for a M_W 6.8 NA plate earthquake in the Georgia basin model is 5.7. For the Greater Vancouver region, the average maximum basin amplification is a factor of 2.9.

A set of 9 shallow scenario M_W 6.8 NA plate earthquakes are simulated in Georgia basin and non-basin structure models to predict long-period ground motions in Greater Vancouver. Figure 10 presents maps of the average PGV and basin amplification of all 9 scenario earthquakes. These maps are considered to provide an estimate of the average peak motion and basin amplification related to a shallow NA plate earthquake within 100 km of Greater Vancouver. The presence of the Georgia basin significantly increases the level of predicted long-period ground motions. For the Georgia basin region as a whole, the average maximum PGV is 8.3 cm/s, related to an intensity of V-VI. The average maximum basin amplification is a factor of 3.4.

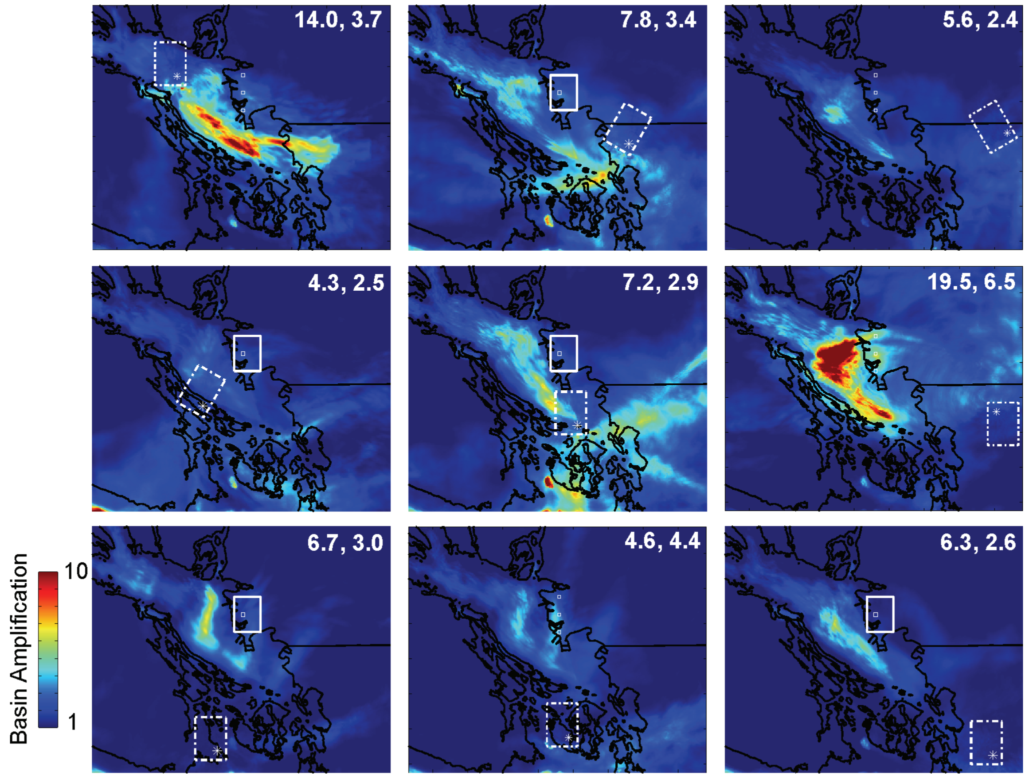

Figure 9. Basin amplification for all 9 shallow scenario earthquakes. Details as in Figure 5.

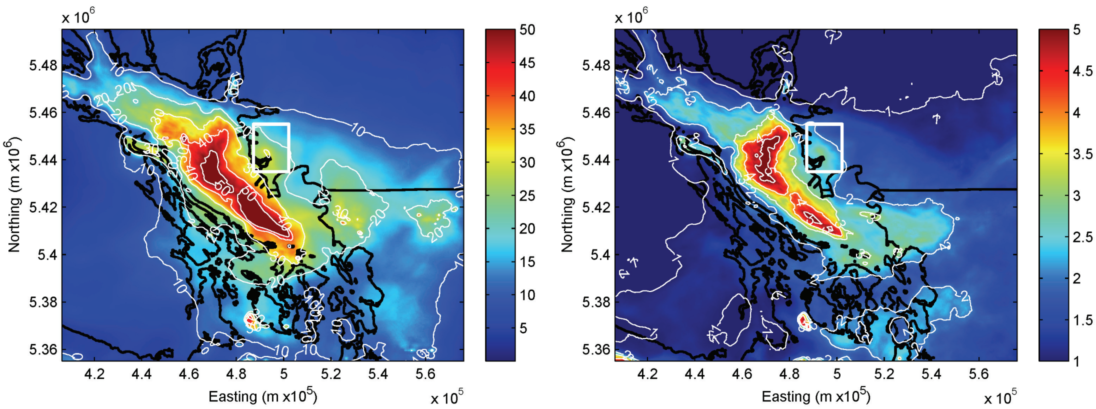

Figure 10. Average PGV (left panel) and basin amplification (right panel) of all 9 shallow scenario earthquakes. Details as in Figure 6.

4. SUMMARY AND CONCLUSIONS

To assess the effects of 3D Georgia basin structure on long-period (> 2 s) ground motion due to large earthquakes within 100 km of Greater Vancouver, numerical 3D FD modeling of viscoelastic wave propagation is carried out. This research provides the first detailed investigation of 3D earthquake ground motion for a sedimentary basin in Canada and represents an important step towards quantifying the effect of the Georgia basin on earthquake ground motion in SW British Columbia. Accuracy of the 3D FD simulations is evaluated by comparing predicted and empirical waveforms of the 2001 M_W 6.8 Nisqually earthquake. Estimates of PGV in the near-source region are biased by a factor of 1.3, whereas in the Georgia basin region the bias between predicted and empirical PGV is a factor of 1.6. Overall, confidence in the use of the Nisqually earthquake source model to simulate large subducting JdF plate scenario earthquakes in the Georgia basin region is achieved.

Large M_W 6.8 scenario earthquakes in both the upper crust of the NA plate and within the subducting JdF plate are simulated within the Georgia basin region with hypocenters in realistic locations based on known seismicity. Shallow NA plate events are characterized here by EW-striking blind-thrust faults which initially rupture at 5 km depth then propagate predominantly N (down-dip). Deep JdF plate earthquakes are characterized by the source process of the 2001 M_W 6.8 Nisqually earthquake: a N-striking steeply E-dipping normal fault event. For all simulations, some general effects are observed consistently when Georgia basin sediments (1.5 km/s < V_P < 5.5 km/s) are included in the 3D structure model. The symmetry of the seismic radiation pattern is distorted and the area of strong ground motion is increased. Surface waves are generated in the SE and NW parts of the basin coincident with steep basin edges in the upper 1 km of the model. The distribution of basin-amplified motion primarily corresponds to the lowest-velocity sediments in the basin model. Overall, stronger and longer ground shaking occurs across Greater Vancouver for earthquakes located S-SW of the city at distances greater than ~80 km, regardless of source depth and rupture style.

Conclusions are limited to the simulations conducted here and are specific to the chosen earthquake locations and rupture style. However, conclusions as to the overall most hazardous deep JdF plate scenario earthquake (within 100 km of Greater Vancouver) are relatively robust since the most-likely locations and rupture style of such an event have been considered here. Overall, this study shows that the presence of 3D Georgia basin structure increases the level of predicted long-period ground shaking.

AKCNOWLEDGEMENT

We thank Robert Kung (NRCAN, Pacific) for GIS support, and Minerva computer support staff at the University of Victoria. Funding provided by National Sciences and Engineering Research Council (NSERC) of Canada, University of Victoria, and Natural Resources Canada. ESS contribution number 2012###.

REFERENCES

Balfour NJ, JF Cassidy, SE Dosso & S Mazzotti, 2011. Mapping crustal stress and strain in southwest British Columbia, *J. Geo. Res.*, **116**, B03314, doi:10.1029/2010JB008003.

Balfour NJ, JF Cassidy & SE Dosso, 2011b. Identifying active structures using double-difference earthquake relocations in southwest British Columbia and the San Juan Islands, WA, *Bull. Seis. Soc. Am.*, 102, 6399-649, doi:10.1785/0120110056.

Cassidy JF, GC Rogers & FA Waldhauser, 2000. Characterization of active faulting beneath the Strait of Georgia, British Columbia, *Bull. Seis. Soc. Am.*, **90**, 1188-1199.

Frankel AD, WJ Stephenson, DL Carver, RA Williams, JK Odom & S Rhea, 2007. Seismic hazard maps for Seattle incorporating 3D sedimentary basin effects, nonlinear site response, and rupture directivity, USGS Open File Report 2007-1175, 77 p.

Frankel AD, WJ Stephenson & D Carver, 2009. Sedimentary basin effects in Seattle, Washington: Ground-motion observations and 3D simulations, *Bull. Seis. Soc. Am.*, **99**, 1579-1611.

Molnar, S., 2011. Predicting earthquake ground motion due to 1D soil layering and 3D basin structure in SW British Columbia, Canada. PhD Thesis, University of Victoria, Victoria, BC, 150p, http://hdl.handle.net/1828/3417.

Molnar, S., J.F. Cassidy, K.B. Olsen, S.E. Dosso and J. He, 2012a. Earthquake ground motion and 3D Georgia basin amplification in SW British Columbia: Deep Juan de Fuca plate events, *Bull. Seis. Soc. Am.*, accepted.

Molnar, S., J.F. Cassidy, K.B. Olsen, S.E. Dosso and J. He, 2012b. Earthquake ground motion and 3D Georgia basin amplification in SW British Columbia: Shallow North America plate events, *Bull. Seis. Soc. Am.*, in prep.

Olsen KB, 1994. Simulation of three-dimensional wave propagation in the Salt Lake Basin, *Ph.D. Thesis*, University of Utah, Salt Lake City, Utah, 157 p.

Olsen, K. B., 2000. Site amplification in the Los Angeles basin from three dimensional modeling of ground motion, *Bull. Seis. Soc. Am.* **90** S77–S94.

Pitarka A, R Graves & P Somerville, 2004. Validation of a 3D velocity model of the Puget Sound region based on modeling ground motion from the 28 February 2001 Nisqually earthquake, *Bull. Seis. Soc. Am.*, **94**, 1670–1689.

Stephenson WJ, 2007. Velocity and density models incorporating the Cascadia subduction zone for 3D earthquake ground motion simulations, Version 1.3: USGS, Earthquake Hazards Ground Motion Investigations, Open-File Report 2007–1348, 24 p.
Wald DJ, TH Heaton & KW Hudnut, 1996. The slip history of the 1994 Northridge, California, earthquake determined from strong-motion, teleseismic, GPS, and leveling data, *Bull. Seis. Soc. Am.*, **86**, S49-S70.
Wald DJ, V Quitoriano, TH Heaton & H Kanamori, 1999. Relationship between Peak Ground Acceleration, Peak Ground Velocity, and Modified Mercalli Intensity in California, *Eq. Spec.*, **15**, 557-564.